

**Placing the Deep Impact Mission into Context:
Two Decades of Observations of 9P/Tempel 1 from McDonald Observatory**

A. L. Cochran¹, E. S. Barker², M. D. Caballero³,
and J. Györgey-Ries¹

1: McDonald Observatory, University of Texas, 1 University Station C1402, Austin,
TX 78712

2: NASA Johnson Space Center, KX/Orbital Debris Program Office, 2101 NASA
Pkwy, Houston, TX 77058

3: Georgia Institute of Technology, Center for Nonlinear Science and School of Physics,
Georgia Institute of Technology, Atlanta, GA 30332

Accepted for Icarus

Abstract

We report on low-spectral resolution observations of comet 9P/Tempel 1 from 1983, 1989, 1994 and 2005 using the 2.7m Harlan J. Smith telescope of McDonald Observatory. This comet was the target of NASA's Deep Impact mission and our observations allowed us to characterize the comet prior to the impact. We found that the comet showed a decrease in gas production from 1983 to 2005, with the decrease being different factors for different species. OH decreased by a factor 2.7, NH by 1.7, CN by 1.6, C₃ by 1.8, CH by 1.4 and C₂ by 1.3. Despite the decrease in overall gas production and these slightly different decrease factors, we find that the gas production rates of OH, NH, C₃, CH and C₂ ratioed to that of CN were constant over all of the apparitions. We saw no change in the production rate ratios after the impact. We found that the peak gas production occurred about two months prior to perihelion. Comet Tempel 1 is a "normal" comet.

Keywords: Comet Tempel 1; Comets, composition; Spectroscopy

1 Introduction

On 4 July 2005 UT, comet 9P/Tempel 1 crashed into the Deep Impact spacecraft. The spacecraft was located in the path of the comet in order for the impact to create a large crater, releasing material from the inside of the nucleus, to enable study of interior ices. In order to understand the changes which were observed, it was necessary to have observations of the comet prior to the impact. In this paper, we detail low-resolution spectroscopic observations obtained of comet 9P/Tempel 1 in its 1983, 1989, 1994 and 2005 apparitions using spectrographs on the 2.7m Harlan J. Smith telescope of McDonald Observatory. The observations of 2005 include some made on the night of impact plus the two nights following the impact.

Comet 9P/Tempel 1 is a Jupiter family comet with a 5.5 year period. Its orbit is such that it has alternating good and poor viewing apparitions. The apparitions 11 years apart have very similar viewing geometry. Over the span of our observations, the perihelion date changed slightly and the perihelion distance moved outwards from 1.49 to 1.51 AU (see Table I). All of our data were obtained pre-perihelion with the exception of the data from 5 and 6 July 2005.

Table I: Orbital Parameters

Year	Perihelion Date	Perihelion Distance (AU)	e	i (degrees)
1983	Jul. 9.797	1.491117	0.520898	10.5571
1989	Jan. 4.443	1.496725	0.519684	10.5462
1994	Jul. 3.314	1.494151	0.520255	10.5518
2000	Jan. 2.617	1.500047	0.518953	10.5413
2005	Jul. 5.348	1.506434	0.517490	10.5303
Data from NASA/JPL's Horizons web interface				

2 Observations

The observations from 1983 were obtained with the Intensified Dissector Scanner (IDS) spectrograph. This spectrograph utilized an intensification chain to rapidly build up the spectrum of two regions 52 arcsec apart and 4×4 arcsec in size. By moving the telescope under computer control, the user could probe multiple positions in the coma. The observations of 1983 have already been published in Cochran *et al.* (1992). Table II includes a log of the circumstances of these observations.

The observations of 1989, 1994 and 2005 were obtained with the Large Cassegrain Spectrograph (LCS), a long-slit CCD spectrograph. The slit was 2 arcsec wide and 150

Table II: The Intensified Dissector Spectrograph Observational Circumstances

Date	R_h (AU)	Δ (AU)	Aperture (km)
16 Feb 83*	2.01	1.22	3532×3532
17 Feb 83*	2.00	1.21	3496×3496
13 Mar 83*	1.87	0.94	4073×4073
14 Mar 83*	1.86	0.93	4056×4056
09 Apr 83*	1.73	0.76	2199×2199
10 May 83	1.60	0.71	2071×2071
12 May 83	1.60	0.72	2077×2077
09 Jun 83*	1.52	0.78	2269×2269
10 Jun 83	1.52	0.79	2280×2280
08 Jul 83	1.50	0.91	2640×2640

* not photometric

arcsec long, with the pixels each subtending 1.28 arcsec on the sky. The slit could be rotated to any arbitrary angle on the sky. Observations typically covered 3000–5700Å at 7Å resolution. Table III includes a log of the circumstances of these observations. We often obtained more than one spectral image at any particular position angle of the slit. In Table III the exposure times are given for these multiple spectra (i.e. “2×1800 sec” indicates 2 spectra of 30 min each or “2700, 1800 sec” indicates a 45 min and 30 min spectrum).

Once the routine reductions were performed for each instrument (flat field, extraction, wavelength calibration and flux calibration for the IDS; bias correction, flat field, wavelength and flux calibration for the LCS) we needed to compute the column densities and production rates for each spectrum. For the IDS, this was performed on the spectra from each individual position on the sky. Since the LCS is a long slit instrument, we would treat each row of the spectral image as a spectrum of a different position within the coma (or sometimes pairs of rows would be binned). First, we subtracted a sky spectrum from each comet spectrum, generally weighting by the strength of the 5577Å night sky O (¹S) line. Next, we removed the solar spectrum which results from the reflection of sunlight from the cometary dust. We used either a solar analogue star spectrum obtained on the same night with the same instrument or, when that was unavailable, a catalog solar spectrum convolved with the instrumental slit profile. A catalog spectrum was always used for the IDS because the solar analogues are too bright. The solar spectrum was typically weighted at five continuum wavelengths in order to match the color of the cometary spectrum. Figure 1 of Cochran *et al.* (1992) demonstrates these steps. For observations of the OH band, we sometimes did not remove the solar or sky spectrum because of the low signal/noise of these observations at the wavelength of OH; removal introduced more noise into the comet spectrum than signal it removed.

Table III: The Large Cassegrain Spectrograph Observational Circumstances

Date	UT Range	R_h (AU)	Δ (AU)	\dot{R} (km/sec)	PA_{sun} (deg)	PA_{slit} (deg)	exposure (sec)
01 Jul 89	09:43 – 10:23	2.23	1.88	10.25	67.5	91	2400
10 Feb 94*	11:06 – 12:16	2.03	1.30	-9.97	101.5	101.5	4200
08 Mar 94	09:03 – 11:09	1.88	0.98	-9.39	83.7	84	2×3600
07 Apr 94	04:55 – 06:49	1.73	0.75	-8.13	14.5	104	2700, 3600
12 Mar 05	07:03 – 08:06	1.87	0.95	-9.26	77.5	90	2×1800
	08:20 – 09:21					347.5	2×1800
	09:34 – 11:11					77.5	3×1800
13 Mar 05*	10:01 – 11:35	1.87	0.94	-9.23	76.1	90	3×1800
06 Apr 05	03:41 – 04:45	1.75	0.77	-8.23	13.0	90	2×1800
	04:55 – 05:56					12	2×1800
	06:07 – 07:09					57	2×1800
	07:19 – 08:20					103	2×1800
07 Apr 05*	03:19 – 04:21	1.74	0.77	-8.18	9.7	90	2×1800
	05:53 – 06:55					9	2×1800
	07:06 – 08:08					99	2×1800
08 Apr 05*	05:03 – 06:06	1.74	0.76	-8.12	6.3	90	2×1800
	06:17 – 07:20					6	2×1800
10 May 05	03:30 – 04:32	1.61	0.71	-5.94	309.3	90	2×1800
	04:52 – 05:55					130	2×1800
	06:05 – 07:07					40	2×1800
12 May 05	02:52 – 03:43	1.60	0.72	-5.77	307.8	90	1200, 1800
08 Jun 05	03:02 – 03:52	1.53	0.78	-3.15	296.1	90	900, 1200
	03:51 – 04:53					116	2×1800
	05:04 – 06:04					26	2×1800
09 Jun 05*	03:16 – 04:48	1.53	0.78	-3.04	295.8	90	1800, 2×700
	04:53 – 06:38					115	1500, 1800
04 Jul 05*	06:07 – 06:28	1.51	0.89	-0.16	291.4	90	2×600
05 Jul 05	03:34 – 04:04	1.51	0.90	-0.04	291.3	45	1800
	04:27 – 04:57					0	1800
	05:09 – 05:39					90	1800
06 Jul 05	03:27 – 03:57	1.51	0.90	0.08	291.1	45	1800
	04:20 – 04:50					0	1800
	04:57 – 05:27					30	1800

* not photometric

PA = Position Angle, measured North through East

Once the sky and solar spectra were removed, we fit a continuum to the region around each cometary emission band, removed the continuum and then integrated the flux above the continuum for each cometary molecular band observed. (Though there should be no continuum left after the removal of the solar spectrum, in reality the color weighting of the solar spectrum is not perfect because there are few true continuum regions. The fitted continuum provides an accurate level to integrate above.) The integrated fluxes were next converted to column densities using the standard efficiency factors listed in Table II of Cochran *et al* (1992). In addition to the molecules listed in that table (CN, C₃, CH, C₂ and NH₂), we used the ‘‘Swings effect’’ calculations of Schleicher and A’Hearn (1988) to derive a fluorescence efficiency for OH and of Kim *et al* (1989) for NH. At this point, for any particular night and slit orientation, we had multiple values of column density as a function of position within the coma. Finally, we converted the data to production rates using the Haser (1957) model and the scale lengths listed in Table IV. We have modified the outflow velocity law of Delsemme (1982) to yield a velocity of 0.85 km/sec at 1 AU (as opposed to the original 0.58 km/sec) to agree with the Giotto Halley results (see discussion in Cochran and Schleicher 1993). The velocity scales as $R_h^{-0.5}$ (R_h = heliocentric distance). When there were multiple slit orientations in the course of a night, we calculated separate production rates for each orientation. Since the slit always contained the optocenter of the comet, each orientation should give the same value of the production rate if it was photometric. The constancy of these values is an excellent indicator of our uncertainties.

Table IV: Adopted Haser Model Scale Lengths

Molecule	Parent Scale length (km)	Daughter Scale length (km)	Reference ^a
OH	2.4×10^4	1.6×10^5	1
NH	5.0×10^4	1.5×10^5	2
CN	1.7×10^4	3.0×10^5	3
C ₃	3.1×10^3	1.5×10^5	3
CH	7.8×10^4	4.8×10^3	4
C ₂ ^b	2.5×10^4	1.2×10^5	3
NH ₂	4.1×10^3	6.2×10^4	

^aReferences – 1: Cochran and Schleicher (1993); 2: Randall *et al.* (1992); 3: Cochran (1986); 4: Cochran and Cochran (1990)

^b C₂ parent scales as $R_h^{2.5}$, all others as R_h^2

Not all of the observations were obtained in photometric weather. The weather is noted in Tables II and III. Since all wavelengths were observed simultaneously, even non-photometric weather yields interesting information because the relative abundances

of the species are unaffected by cloud (clouds have been shown to be grey (Wing 1967)). Similarly, all positions of a single spectral image of the LCS are obtained simultaneously, so the spatial information is meaningful even when cloudy. When there was more than one spectral image at a position and the weather was not photometric, the fainter (more cloudy) image was shifted upwards to align with the brighter image. In all cases except on 4 July 2005, individual spectral images were processed separately up until the Haser model was fit; for 4 July, the spectra were averaged first to increase the signal/noise (see discussion later about the use of the Haser model for the July 2005 data).

Table V lists the Haser model production rates we derived from the 1983 data with the IDS. These are fit to the same data we reported in Cochran *et al.* (1992) except that we have recalculated the Haser model production rates using the higher outflow velocities described above. We report production rates for CN, C₃, C₂, CH and one data point for NH₂. Note that the CN production rate for 9 April 1983 reported in Cochran *et al.* (1992) was mis-typed. The value in that paper should have been $\log Q(\text{CN})=24.96$ instead of 24.21. With the higher velocity used in this work, we get $\log Q(\text{CN})=25.13$.

Tables VI and VII give the production rates for the data from 1989, 1994 and 2005. We list the production rates for each molecule observed (OH, NH, CN, C₃, CH and C₂) on each night and at each slit orientation, as well as the binning in the spatial direction (e.g. a bin of 2 means the effective slit was 2.56 arcsec spatially and 2 arcsec wide) and the number of positions which went into the Haser model. All of the underlying band intensities and column densities for these positions will be archived in the Planetary Data System's Small Bodies Node (PDS SBN).

The data vary in quality as weather and cometary brightness changed over an apparition. Also, some molecules such as CN are intrinsically easier to observe because they are strong lines; molecules such as CH are generally quite weak. OH, while generally strong, is affected by low quantum efficiency of the detector at 3080Å and large atmospheric extinction. Figure 1 shows examples of the column densities from individual coma positions for these three molecules under excellent and poorer conditions. The Haser model fits are shown with the data.

Inspection of this figure shows several salient features. Even under the poorer conditions of 13 March 2005, the CN data show a clear trend. However, the Haser model does not fit these data well. Recall that we are using fixed scale length values and not trying to fit the data. This shows a weakness in the model but we use this approach for inter-comparability of these data and those for other comets. We often see that the gas distribution for any molecule is dependent on the orientation of the slit, with different profiles on either side of the optocenter. The Haser model does not take asymmetries into account.

Table V: IDS Production Rates

Date	log Q(CN)	Npts	log Q(C ₃)	Npts	log Q(CH)	Npts	log Q(C ₂)	Npts	log Q(C ₂)	Npts	log Q(NH ₂)	Npts
	(sec ⁻¹)		(sec ⁻¹)		(sec ⁻¹)		$\Delta v = 1$ (sec ⁻¹)		$\Delta v = 0$ (sec ⁻¹)		(sec ⁻¹)	
16 Feb 83	24.03	2								0		
17 Feb 83	24.48	2								0		
13 Mar 83	24.86	4	24.16	2					25.12	4		
14 Mar 83	24.53	18	23.45	6					24.86	14		
09 Apr 83	25.38	18	24.38	16			25.26	15	25.10	15		
10 May 83	25.14	16	24.42	14	25.23	6	25.06	16	25.11	16	24.75	2
12 May 83	25.03	6	24.31	6	25.26	3	24.97	6	25.01	6		
09 Jun 83	24.70	4	23.77	2					24.82	4		
10 Jun 83	25.00	22	24.30	14			25.09	15	25.01	19		
08 Jul 83	24.71	4	24.04	4			24.65	4	24.76	4		

Table VI: LCS Production Rates (part 1)

Date	PA (deg)	log Q(OH) (sec ⁻¹)	bin	Npts	log Q(NH) (sec ⁻¹)	bin	Npts	log Q(CN) (sec ⁻¹)	bin	Npts	log Q(CH) (sec ⁻¹)	bin	Npts
1 Jul 89	91							24.17	2	13			
10 Feb 94	101.5	26.44	2	50	24.84:	2	46	24.38	1	113	24.66:	2	34
8 Mar 94	84	27.03	2	121	25.15	2	110	24.63	1	243	25.31:	2	116
7 Apr 94	104	27.23	1	241	25.34:	1	241	24.88	1	247	25.06	2	97
12 Mar 05	90	26.57:	3	48	24.81:	3	44	24.38	3	62	24.86:	3	40
	347.5	26.51:	3	31	24.70:	3	42	24.33	3	70	24.92:	3	33
	77.5	26.53:	3	41	24.83:	3	64	24.31	3	93	24.75:	3	39
13 Mar 05	90	26.86:	2	102	25.26:	2	104	24.43	2	133	25.32:	2	119
6 Apr 05	90	26.83	2	79	25.10	2	109	24.65	2	118	24.83:	2	84
	12	26.97	2	103	25.13	2	116	24.67	2	122	24.97:	2	87
	57	26.94	2	106	25.11	2	122	24.66	2	112	24.82:	2	46
	103	26.93	2	115	25.08	2	120	24.63	2	123	24.69:	2	55
7 Apr 05	90	26.86:	2	102	25.15:	2	105	24.71	2	125	25.09:	2	102
	9	27.02	2	106	25.16	2	110	24.69	2	123	24.90:	2	81
	99	27.03	2	111	25.17:	2	102	24.70	2	124	24.97:	2	85
8 Apr 05	90	26.97	2	108				24.64	2	119	24.90:	2	79
	6	26.85	2	106				24.62	2	121	25.02:	2	65
10 May 05	90	27.07	2	111	25.29	2	112	24.90	1	250	25.14	2	89
	130	27.00	2	113	25.23	2	111	24.85	1	248	25.07	2	76
	40	26.91	2	49	25.24:	2	84	24.89	1	245	25.13	2	75
12 May 05	90	27.08	2	117	25.26	2	114	24.91	1	248	25.12:	2	95
8 Jun 05	90	26.78	1	85	25.31	1	121	24.75	1	248	24.95:	1	84
	116	26.80	1	122	25.25	1	123	24.71	1	246	24.76:	1	79
	26	26.62:	1	87	25.16	1	117	24.73	1	247	24.63:	1	52
9 Jun 05	90	26.85:	1	119	25.29:	1	173	24.75	1	371			
	115	26.78	1	55	25.27	1	111	24.59	1	246			
4 Jul 05	90							24.62	1	43			
5 Jul 05	45	27.06:	1	76	25.27	1	105	24.92	1	118	25.09:	1	79
	0	27.14:	1	63	25.22	1	101	24.86	1	118	25.04:	1	82
	90	27.24:	1	38				24.96	1	113	25.03:	1	74
6 Jul 05	45	27.02:	2	35	25.27	2	53	24.92	1	114	25.00:	2	48
	0	27.04:	2	32	25.19	2	48	24.86	1	114	24.99:	2	46
	30	26.86:	2	17	25.16:	2	47	24.82	1	106	24.91:	2	43

Note – values with a : after them are very uncertain due to scatter; good to a factor of 2

For OH and CH, even on a good night, there is much more scatter than for CN. Indeed, one can question how to interpret the “fit” to the data for CH on 13 March 2005! We use a Monte Carlo approach to quantifying our errors. Each individual column density has an error based on the Poisson noise and on the quality of the data (weather, airmass, strength of the feature). We take the original data and alter each individual column density by selecting from a normal distribution with an initial width of the S/N at the peak and varying the width to account for S/N decrease as we are farther from optocenter. Then we rerun the model and produce a new fit and production rate. By repeatedly altering the data and refitting them, we build up a picture of how errors in individual data points affect the fit. After 100 such runs, we find that the data for CH on 13 March 2005 yields the same fit extremely reliably ($\log Q(\text{CH}) = 25.32 \pm 0.02$). This very small error bar is not the result of the data being high quality (in this case they are not) but is the result of us having 119 individual measures of the column density and, thus, the errors in individual points do not change the overall shape of the gas distribution. It is, of course, a statistical error and does not include any systematic uncertainties such as calibration problems or incorrect scale lengths or fluorescence efficiencies. The innermost points for CH on this night are probably highly affected by uncertainties in the removal of the continuum around this very weak feature. The dust continuum declines faster with cometocentric distance than does the gas, so the effects of the continuum are strongest near the optocenter.

In general, most of the CN data look closer in quality to the 8 June 2005 data than to the 13 March 2005 data (one of our poorest nights). The weaker features such as CH are rarely of very high quality. Low quality, marginal data points are flagged in the production rate tables. The OH data quality depends on the airmass (so is of lower quality near the end of the 2005 observations). The overall error bars are best judged by looking at the scatter in the column densities and of the production rates derived for different slit orientations on a single night. Interested readers can obtain those from the PDS SBN. The scatter ranges from a few percent (e.g. 8 June 2005 CN) to large factors (e.g. 13 March 2005 CH - but note that even with the scatter in CH, we generally derived consistent production rates from different slit orientations). For C_2 , comparison of the results from the $\Delta v = 1$ and $\Delta v = 0$ complexes give a good estimate of the accuracy. When multiple position angles of the slit were used, consistency of the production rates is also a good indicator of accuracy. The CN, C_3 , and C_2 features are always the most certain values and are probably good 0.1 dex. Of course, on non-photometric nights, the *absolute* values are not accurate but the *relative* values are. The other systematic error is the fact that the Haser model cannot always fit the profiles (NH is generally badly fit). This error is hard to quantify. The Haser model, with published scale lengths, was used as a standard tool for comparison.

Table VII: LCS Production Rates (part 2)

Date	PA	log Q(C ₃)	bin	Npts	log Q(C ₂)	bin	Npts	log Q(C ₂)	bin	Npts
	(deg)	(sec ⁻¹)			$\Delta v = 1$ (sec ⁻¹)			$\Delta v = 0$ (sec ⁻¹)		
1 Jul 89	91									
10 Feb 94	101.5	23.78	2	47	24.30:	2	47	24.54	1	109
8 Mar 94	84	23.94	2	79	24.58	2	117	24.80	1	244
7 Apr 94	104	24.33	1	232	24.92	1	245	24.98	1	249
12 Mar 05	90	23.99	3	48	24.34:	3	53	24.18	3	58
	347.5	23.90	3	54	24.32:	3	33	24.13	3	58
	77.5	23.88:	3	63	24.30:	3	54	24.04:	3	70
13 Mar 05	90	24.34	2	131	24.64	2	75	24.50	2	131
6 Apr 05	90	24.19	2	107	24.72	2	105	24.75	2	105
	12	24.17	2	107	24.73	2	107	24.77	2	119
	57	24.10	2	99	24.77	2	107	24.74	2	106
	103	24.10	2	98	24.71	2	111	24.75	2	115
7 Apr 05	90	24.21	2	109	24.81	2	99	24.81	2	113
	9	24.15	2	104	24.80	2	107	24.81	2	116
	99	24.15	2	104	24.80	2	104	24.82	2	109
8 Apr 05	90	23.90	2	41				24.77	2	112
	6	23.84	2	74				24.73	2	118
10 May 05	90	24.05	1	114	24.91	1	246	25.00	1	246
	130	24.11	1	169	24.88	1	242	24.98	1	244
	40	24.02	1	72	24.88	1	122	25.00	1	248
12 May 05	90	24.06	1	140	24.91	1	239	25.03	1	249
8 Jun 05	90	24.11	1	194	24.87	1	247	24.85	1	248
	116	24.06	1	202	24.80	1	247	24.83	1	247
	26	24.04	1	198	24.77	1	243	24.82	1	247
9 Jun 05	90	24.12	1	303	24.85	1	367	24.84	1	371
	115	24.02	1	174	24.69	1	238	24.77	1	248
4 Jul 05	90	24.30:	1	44	24.49	1	43	24.71	1	55
5 Jul 05	45	24.14	1	107	24.96	1	117	24.95	1	118
	0	24.11	1	101	24.91	1	116	24.92	1	115
	90	24.21:	1	97	24.87	1	114	24.99	1	118
6 Jul 05	45	24.13	1	107	24.95	1	117	24.94	1	115
	0	24.11	1	101	24.92	1	115	24.92	1	115
	30	24.07:	1	97	24.88	1	113	24.89	1	118

Note – values with a : after them are very uncertain due to scatter; good to a factor of 2

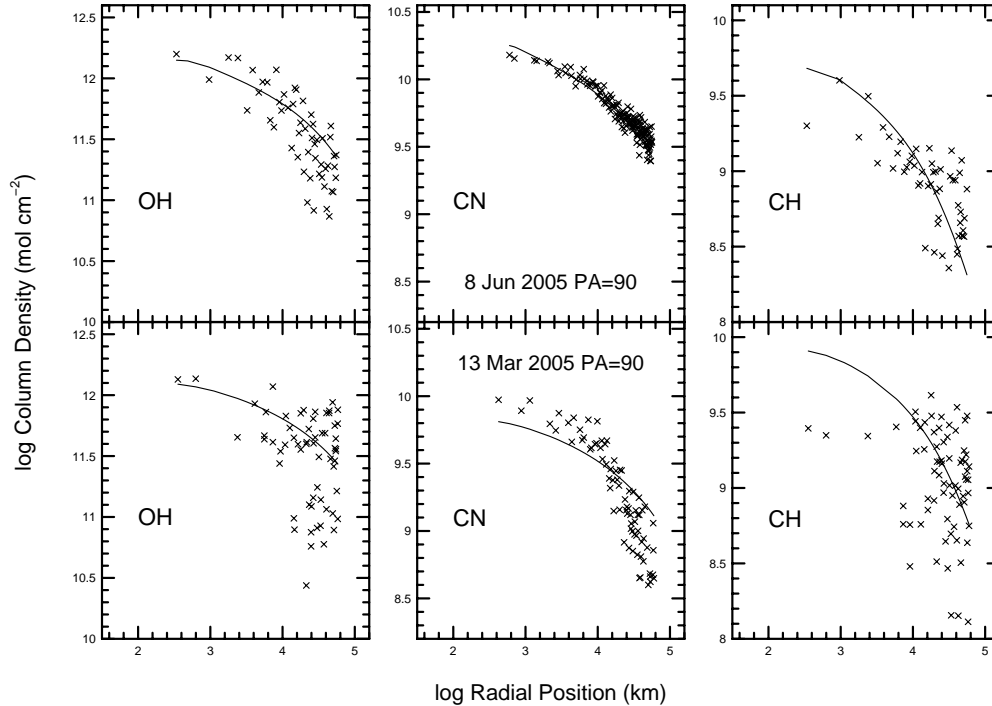


Figure 1: The column densities as a function of cometocentric distance are shown for OH, CN and CH on 8 June 2005, when it was clear, and 13 March 2005, when it was not. The Haser model fits are also plotted. All boxes in a row are for the same date, marked in the middle panel. Clearly, the data are better for some molecules than for others and are better on 8 June than on 13 March. Also, the Haser model does not always fit. See the text for a discussion of the errors.

3 Trends in the Data

We have plotted the production rates of each molecule as a function of heliocentric distance for nights on which it was clear. These are shown in Figure 2. Several features are apparent from this plot. First, the systematic errors can be estimated from the agreement between data points at the same heliocentric distance in the 2005 data set. As would be expected, the CN values are much more consistent than the CH values. All of the data, except for the data from the two post-impact nights, were obtained pre-perihelion. However, the peak of the gas production does not occur at the smallest heliocentric distances for any molecule. Instead, the production peaks prior to perihelion, when the comet is at about 1.6 AU, and then declines (the CH and NH data are not of sufficient accuracy to judge their behavior). This behavior was first noted in data from 1983 by Osip *et al.* (1992).

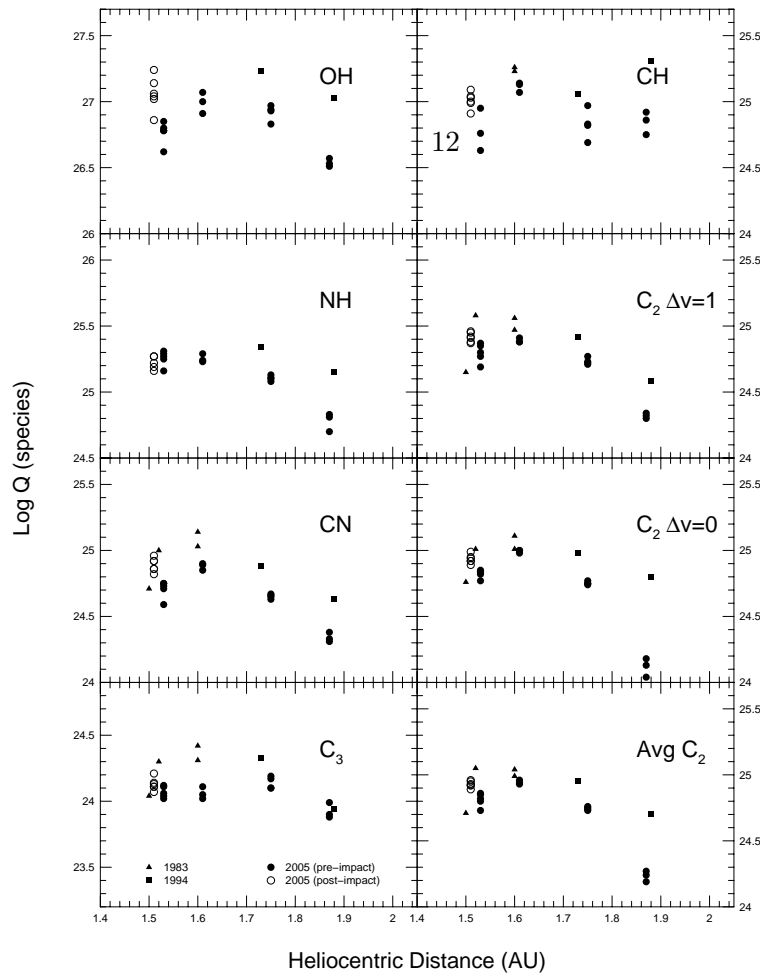


Figure 2: The production rates for nights with no cloud are shown. Data from 1983 are denoted with triangles, from 1994 with squares and from 2005 with circles. The open circles are the data from 5 and 6 July 2005, or post-impact. Note that the peak column densities are well before perihelion (excluding the post-impact data). This is true for all three apparitions. The comet was systematically less productive in 2005.

There is a significant offset in the production of all of the species from 1983/1994 to 2005 (unfortunately the weather was not cooperative enough to determine if there is an offset from 1983 to 1994). For all molecules, the gas production was higher in 1983/1994 than in 2005. This was also reported by Schleicher (2007). The magnitude of the decrease is different for different molecules. We find that, at its peak, CN decreased by a factor of 1.6, C_3 by 1.8, CH by 1.4, and C_2 by 1.3. We were not able to observe NH or OH in 1983 and did not observe the comet in clear weather at its peak in 1994. By extrapolating a linear trend for the 1994 data for clear nights, we can estimate a decrease of OH by a factor of 2.7 and of NH by a factor of 1.7. The numbers are slightly different than those factors seen by Schleicher (2007), who saw decreases of OH by a factor of 2.5, NH and CN by 1.9, C_3 by 1.5 and C_2 by 1.4. Our C_3 data at 1.6 AU looks a little low, so may explain the difference in our and Schleicher's C_3 decrease factor. We have no explanation why the C_3 is low except that the model does not fit the gas distribution as well as at other times and thus may be giving a false low value.

The data are somewhat sparse, with clumps of data at each of several heliocentric distances. The data were obtained approximately monthly, based on the lunar cycle, and the viewing geometry was similar in the 1983, 1994 and 2005 apparition. There is a suggestion in Fig. 2 that the behavior of the gas production of some species with heliocentric distance was not the same in all three apparitions. In particular, C_2 , NH and perhaps CN seemed to have higher production rates at 1.75 AU relative to 1.9 AU in the 2005 apparition than in 1994. However, the data were not of the same quality in 1983 or 1994 as 2005 so this suggestion is only tentative.

We can utilize all of the data, including the nights with clouds, to look at gas production ratios. These ratios have been used by many authors to characterize comets as “normal” or “depleted” (A’Hearn *et al.* 1995; Cochran *et al.* 1992; Newburn and Spinrad 1984; Fink and Hicks 1996). Figure 3 shows the production rates for OH, NH, C_3 , CH, and C_2 ratioed to that for CN, including all of the data. Inspection of this plot shows that these ratios were constant with heliocentric distance with the possible exception of CH/CN. However, the CH data are not as high quality as other data since this feature is extremely weak. For the other species, while there are obvious outliers, there appears to be no change in the production rate ratios with heliocentric distance. The mean values are denoted in each panel of the plot. Tempel 1 looks to be a normal comet when compared with the values found by Cochran *et al.* (1992). Since other groups use slightly different scale lengths and fluorescence efficiencies, it is not easy to compare with them. However, there has never been any evidence that Tempel 1 is not normal.

As noted above, the gas production rates of the various species decreased from 1983 to 2005 and different species decreased by various amounts. Despite that, Fig. 3 shows no evidence for a change in the ratios of species. However, only OH appeared to decrease from 1983 to 2005 by a factor much different than that for CN so it is not surprising that the ratios did not change; for OH, there are not many points other than in 2005. There are far more data points from 2005 than from either 1983 or 1994 so the 2005 data dominate the average values shown in each panel. To check for subtle changes in the ratios, we averaged each production rate ratio by year. These are listed in Table VIII. Inspection of this Table shows that there are no real relative compositional differences seen, within the errors.

The data from the impact and post-impact are the circles at 1.5 AU. The clear circle is the night of impact. We see that these production rate ratios from impact and after do not look any different than the data from any other earlier night. Thus, we can conclude that the material populating the coma and observed in our post-impact spectra has the same relative composition as the normal coma material.

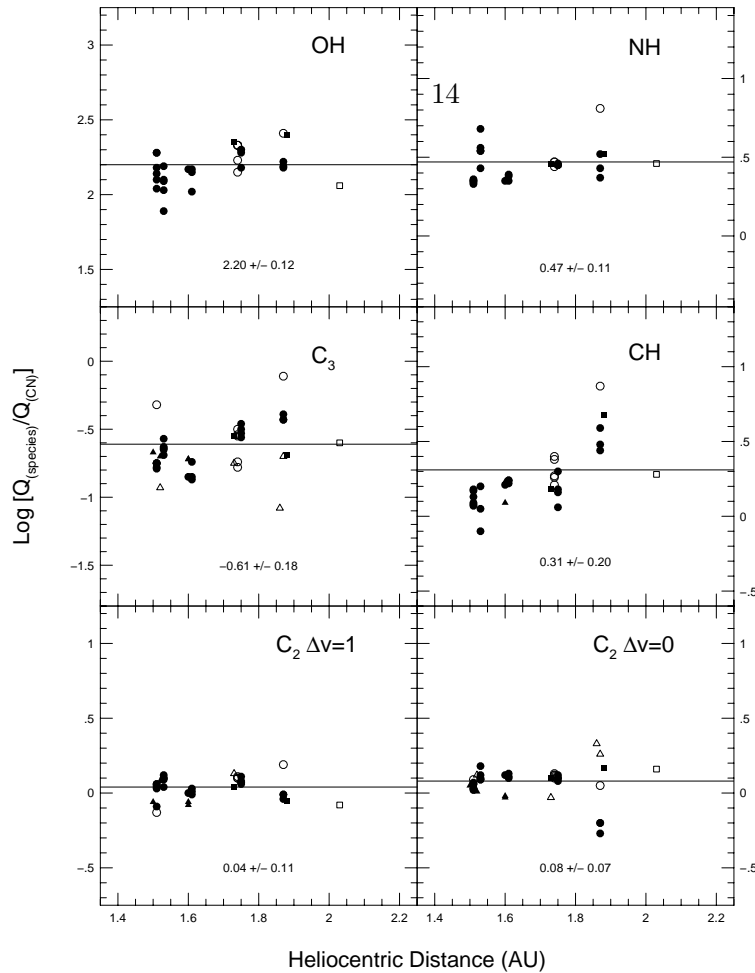


Figure 3: The production rates of various species are ratioed to the production rate of CN and shown versus heliocentric distance. These ratios do not change with heliocentric distance, with the possible exception of CH. The average values are noted in each panel. Data from 1983 are triangles, from 1994 are squares and from 2005 are circles. Filled symbols are clear nights; open symbols are cloudy nights. The circles at 1.5 AU are the nights of 4–6 July 2005 UT, or the night of impact and onwards. The comet looks the same post-impact as before.

Table VIII: Production Rate Ratios by Year

Year	$\log \frac{Q(OH)}{Q(CN)}$	$\log \frac{Q(NH)}{Q(CN)}$	$\log \frac{Q(C_3)}{Q(CN)}$	$\log \frac{Q(CH)}{Q(CN)}$	$\log \frac{Q(C_2)}{Q(CN)}$ $\Delta v = 1$	$\log \frac{Q(C_2)}{Q(CN)}$ $\Delta v = 0$
1983			-0.77 ± 0.14	0.17 ± 0.10	0.01 ± 0.10	0.11 ± 0.14
1994	2.29 ± 0.18	0.48 ± 0.03	-0.61 ± 0.07	0.44 ± 0.26	-0.03 ± 0.06	0.14 ± 0.04
2005	2.19 ± 0.12	0.47 ± 0.11	-0.58 ± 0.18	0.30 ± 0.20	0.05 ± 0.07	0.07 ± 0.10
All	2.20 ± 0.12	0.48 ± 0.11	-0.61 ± 0.18	0.30 ± 0.20	0.04 ± 0.07	0.08 ± 0.11

4 Discussion

The goal of the Deep Impact spacecraft mission was to study the interior of a comet by excavating material from deep within the nucleus. Groussin *et al.* (2007) analyzed IR spectra obtained from the flyby spacecraft to determine that the thermal inertia was low, “most probably $< 50 \text{ W K}^{-1} \text{ m}^{-2} \text{ s}^{1/2}$ ”. This low thermal inertia implies that the sublimation of volatiles generally occurs close to the surface. The exact depth of the crater produced by the impact is unknown, but probably included “deep” materials (Schultz *et al.* 2007).

This unique event was monitored by observatories world-wide as a complement to the data which were obtained by the spacecraft (Meech *et al.* 2005). In order to understand the event, it was necessary to place the impact monitoring observations into the context of the usual behavior of this comet. Our observations, reported in this paper, allow not only for an understanding of the state of the comet at the time of the impact, but also allow for an understanding of the natural changes we see in this comet.

Comet Tempel 1 rotates relatively slowly, with a rotation period of 1.701 ± 0.014 days (A’Hearn *et al.* 2005). Thus, our observations on a single night and a single slit orientation were never more than 5% of the rotation period. Thus, even if there had been a strong active region, it would not change position much relative to our slit during a single night. Major jets show up as moving “bumps” in the gas distribution as the material flows outward (Cochran and Trout 1994). Observations on subsequent nights might have viewed different regions, but we do not see any differences from night-to-night in our data. In addition to the smoothly varying rotational modulation, the comet would undergo sporadic outbursts (A’Hearn *et al.* 2005; Meech *et al.* 2005; Farnham *et al.* 2007). However, according to Table 1 of Farnham *et al.*, there were no outbursts on our dates of observations. Thus, the outbursts would have little affect on our observations.

Therefore, we can use our observations to comment on the properties of the gas production of comet Tempel 1 during the season leading up to the impact and also over the preceding two decades. Overall, comet Tempel 1 is a moderate producer of gas. IR observations with the Deep Impact spacecraft found that water ice “is restricted to three discrete and relatively small areas” (Sunshine *et al.* 2007) (this is not altogether consistent with the conclusion of Ferrin (2007) that Tempel 1 is a young comet). Our values for the production rates of the various optically observed emissions are in good agreement with Schleicher (2007), with small differences due to differences in fluorescence efficiencies, scale lengths and outflow velocities used in the modeling. Lara *et al.* (2006) also observed comet Tempel 1 during 2005. Their derived production rates are lower than ours and Schleicher’s by a factor of a few for C_2 , C_3 , and CN, the species they observed. We cannot explain this difference.

Within the error bars, the comet produced the same *relative* amounts of all of the

species that are in our bandpass for the three well observed apparitions, even while the overall amount of gas was decreasing. We see the same abundance ratios in the spectra from 4 July 2005, the night of impact. The impact was an inherently non-steady state event while the Haser model assumes steady state production. Therefore, the production rates for July 2005 must be used cautiously. On 4 July, the observations were obtained with the first 40 minutes after the impact so ejecta from the impact would only affect our inner few pixels (at 0.5 km sec^{-1} outflow, gas from the crater will flow outwards 1200km in 40 minutes, or less than 1 pixel). The outer part of the slit would still have the ambient signal and this is what we would be measuring predominantly. By 24 hours later, the ejected material would have traveled across our slit. The increase in production resulted from freshly exposed surface (Jackson *et al.* 2008, in preparation). Inspection of the gas distribution shows that within our slit, the gas distribution has the same general shape on 4 through 6 July as on other nights (Fig 4). Rauer *et al.* (2006) found a "bump" of material in observations from 4 and 5 July. However, along the Sun-comet line (their Fig. 4), their profiles look the same for the two nights. Within the scatter, ours do too, as seen in Fig. 4. We did not have a similarly oriented slit angle on 6 July. Thus, while a Haser model production rate does not account for the impulsive nature of the event, it allows for comparison with previous data. The freshly released material has the same relative composition as the ambient material. As long as the impact excavated material deep enough that it reached fresh, unprocessed material, the implication of our findings is that the comet does not differentially lose one kind of ice versus another as it passes through the inner Solar System repeatedly. This also means that prior studies of cometary composition via observations of the normal coma emissions are probing the original composition of these primitive bodies.

This rich data set, which spans more than two decades and four apparitions allows us to look at secular changes in the comet. We find that the total gas abundances declined from 1983 to 2005, with decreases of factors of 1.3–2.7, depending on the species. This is in good agreement with Schleicher (2007). Except in cases where a comet was totally disrupted (e.g. 1999 S4 (LINEAR)) or its orbit changed significantly (e.g. 81P/Wild 2), such large changes of gas production have not been seen before. The simplest explanation is that some region which was active on the surface of the comet in 1983 was not well illuminated in 2005. However, A'Hearn *et al.* (2005) found that the obliquity of the comet was only 11° and the viewing geometry was very similar in 1983, 1994 and 2005. Thus, the only way the illumination of a particular active region could change would be if that active region was very near a pole. This cannot be confirmed with the flyby data since the encounter period was very short. Such a polar jet has been seen in comet Borrelly (Soderblom *et al.* 2002). Other mechanisms, such as the "sealing" of an active region from the fall-back of dust after perihelion, cannot be ruled out.

We found that the gas production was not symmetric around perihelion but peaked almost two months prior to perihelion. Because we observed only at monthly intervals, we cannot comment on whether different species peaked at different times, something that

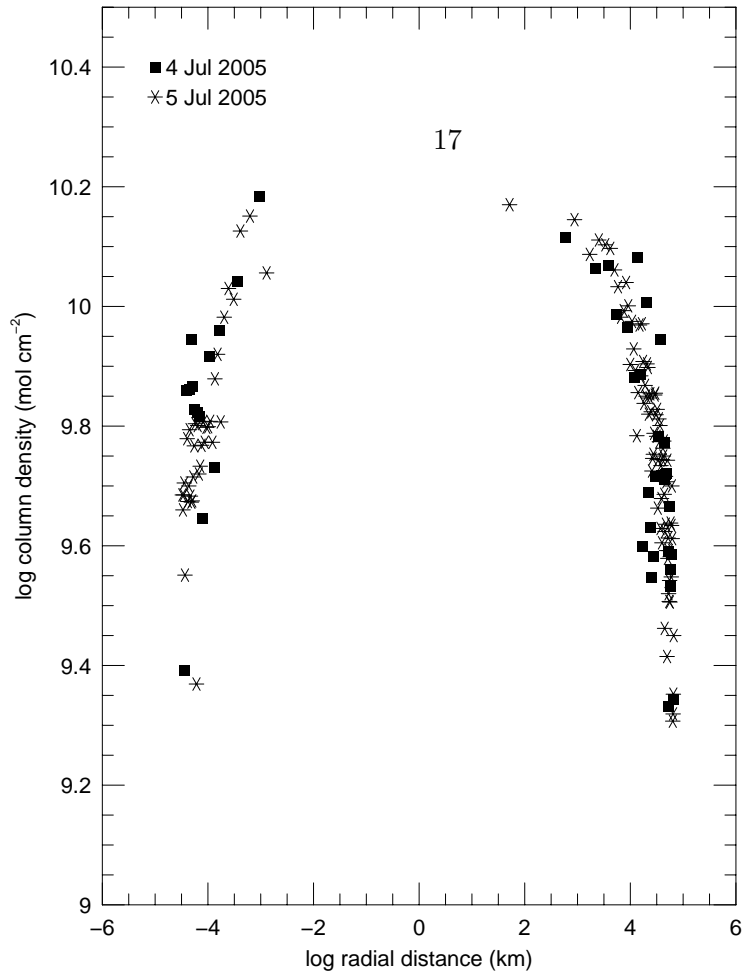


Figure 4: The column densities from 4 and 5 July 2005 UT are compared, with the data from 4 July scaled upwards to match the level of the data from 5 July. Note that the distribution of the gas with cometocentric distance is not the same on the east (negative direction) and west sides of the comet. The slit position angle was 20 degrees off of the extended heliocentric radius vector so the slit is essentially along the Sun-comet line. Within the scatter of the 4 July data, there are no difference in the profiles for 4 and 5 July on either side of the optocenter.

was noted by Schleicher (2007). Such asymmetries are common in cometary activity and generally indicate that small regions of the surface are active and see changing illumination in the course of their orbit. Indeed, as noted above, the Deep Impact spacecraft observations did not observe distinct icy regions as sources of the activity.

Overall, we find that comet Tempel 1 has abundance patterns which are similar to the vast majority of comets and can be classified as a “normal” comet. These abundance patterns do not change with depth, as evidenced from the post-impact spectra. Therefore, as this comet continues to evolve, it is unlikely to change its abundances patterns.

5 Summary

Our main findings are that:

- The relative abundances of different gas species are the same, within the errors, for all three apparitions.
- The comet showed a generalized decrease in activity from the 1983 apparition to the 2005 apparition. The amount of decrease varied, depending on the species, from a factor of 1.3 to a factor of 2.7.
- The production of gas peaks more than a month prior to perihelion.
- Comet 9P/Tempel 1 is like the great majority of comets with “normal” gas abundance ratios.

Deep Impact was a unique experiment to explore the interior of a comet by blasting free material and analyzing this newly released material. In this paper, we have described two decades of observations using spectrographs at McDonald Observatory. These observations allow for placing the Deep Impact results into context with the normal behavior of this comet.

Acknowledgments

This research was supported by NASA Grant NNG04G162G and predecessor grants. McDonald Observatory is operated by The University of Texas at Austin.

References

- A'HEARN, M. F., M. J. S. BELTON, W. A. DELAMERE, J. KISSEL, K. P. KLAASEN, L. A. MCFADDEN, K. J. MEECH, H. J. MELOSH, P. H. SCHULTZ, J. M. SUNSHINE, P. C. THOMAS, J. VEVERKA, D. K. YEOMANS, M. W. BACA, I. BUSKO, C. J. CROCKETT, S. M. COLLINS, M. DESNOYER, C. A. EBERHARDY, C. M. ERNST, T. L. FARNHAM, L. FEAGA, O. GROUSSIN, D. HAMPTON, S. I. IPATOV, J.-Y. LI, D. LINDLER, C. M. LISSE, N. MASTRODEMOS, W. M. OWEN, J. E. RICHARDSON, D. D. WELLNITZ, AND R. L. WHITE 2005. Deep Impact: Excavating Comet Tempel 1. *Science* **310**, 258–264.
- A'HEARN, M. F., R. L. MILLIS, D. G. SCHLEICHER, D. J. OSIP, AND P. V. BIRCH 1995. The ensemble properties of comets: Results from narrowband photometry of 85 comets, 1976–1992. *Icarus* **118**, 223–270.
- COCHRAN, A. L. 1986. A reevaluation of the Haser model scale lengths in comets. *A. J.* **90**, 2609–2614.
- COCHRAN, A. L., E. S. BARKER, T. F. RAMSEYER, AND A. D. STORRS 1992. The McDonald Observatory Faint Comet Survey: Gas production in 17 comets. *Icarus* **98**, 151–162.
- COCHRAN, A. L. AND W. D. COCHRAN 1990. Observations of CH in comets P/Brosen-Metcalf and P/Halley. In *Workshop on Observations of Recent Comets (1990)* (W. F. Huebner, P. A. Wehinger, J. Rahe, and I. Konno, Eds.) pp. 22–27 Southwest Research Institute San Antonio, TX.
- COCHRAN, A. L. AND D. G. SCHLEICHER 1993. Observational constraints on the lifetime of cometary H₂O. *Icarus* **105**, 235–253.
- COCHRAN, A. L. AND A. P. TROUT 1994. The gas distribution of comet halley and its relation to the nucleus rotation. *A. J.* **108**, 1471–1475.
- FARNHAM, T. L., D. D. WELLNITZ, D. L. HAMPTON, J.-Y. LI, J. M. SUNSHINE, O. GROUSSIN, L. A. MCFADDEN, C. J. CROCKETT, M. F. A'HEARN, M. J. S. BELTON, P. SCHULTZ, AND C. M. LISSE 2007. Dust coma morphology in the Deep Impact images of comet 9P/Tempel 1. *Icarus* **187**, 26–40.
- FERRIN, I. 2007. Secular light curve of comet 9P/Tempel 1. *Icarus* **187**, 326–331.
- FINK, U. AND M. D. HICKS 1996. A survey of 39 comets using CCD spectroscopy. *Ap. J.* **459**, 720–743.
- GROUSSIN, O., M. F. A'HEARN, J.-Y. LI, P. C. THOMAS, J. M. SUNSHINE, C. M. LISSE, K. J. MEECH, T. L. FARNHAM, L. M. FEAGA, AND W. A. DELAMERE 2007. Surface temperature of the nucleus of comet 9P/Tempel 1. *Icarus* **187**, 16–25.

- HASER, L. 1957. Distribution d'intensité dans la tête d'une comète. Liege Inst. Astrophysics Reprint No. 394.
- KIM, S. J., M. F. A'HEARN, AND W. D. COCHRAN 1989. NH emissions in comets: Fluorescence vs collisions. *Icarus* **77**, 98–108.
- LARA, L. M., H. BOEHNHARDT, R. GREDEL, P. J. GUTIÉRREZ, J. L. ORTIZ, R. RODRIGO, AND M. J. VIDAL-NUÑEZ 2006. Pre-impact monitoring of comet 9P/Tempel 1, the Deep Impact target. *Astr. and Ap.* **445**, 1151–1157.
- MEECH, K. J. AND 208 ADDITIONAL AUTHORS 2005. Deep Impact: Observations from a worldwide Earth-based campaign. *Science* **310**, 265–269.
- NEWBURN, R. L. AND H. SPINRAD 1984. Spectrophotometry of 17 comets. I. The emission features. *A. J.* **89**, 289–309.
- OSIP, D. J., D. G. SCHLEICHER, AND R. L. MILLIS 1992. Comets: Groundbased observations of spacecraft mission candidates. *Icarus* **98**, 115–124.
- RANDALL, C. E., D. G. SCHLEICHER, R. G. BALLOU, AND D. J. OSIP 1992. Observational constraints on molecular scalelengths and lifetimes in comets. *Bull. AAS* **24**, 1002.
- RAUER, H., M. WEILER, C. STERKEN, E. JEHIN, J. KNOLLENBERG, AND O. HAINAUT 2006. Observations of CN and dust activity of comet 9P/Tempel 1 around Deep Impact. *Astr. and Ap.* **459**, 257–263.
- SCHLEICHER, D. G. 2007. Deep Impact's target comet 9P/Tempel 1 at multiple apparitions: Seasonal and secular variations in gas and dust. *Icarus* **190**, 406–422.
- SCHLEICHER, D. G. AND M. F. A'HEARN 1988. The fluorescence of cometary OH. *Ap. J.* **331**, 1058–1077.
- SCHULTZ, P. H., C. A. EBERHARDY, C. M. ERNST, M. F. A'HEARN, J. M. SUNSHINE, AND C. M. LISSE 2007. The Deep Impact oblique impact cratering experiment. *Icarus* **190**, 295–333.
- SODERBLOM, L. A., T. L. BECKER, G. BENNETT, D. C. BOICE, D. T. BRITT, R. H. BROWN, B. J. BURATTI, C. ISBELL, B. GIESE, T. HARE, M. D. HICKS, E. HOWINGTON-KRAUS, R. L. KIRK, M. LEE, R. M. NELSON, J. OBERST, T. C. OWEN, M. D. RAYMAN, B. R. SANDEL, S. A. STERN, N. THOMAS, AND R. V. YELLE 2002. Observations of comet 19P/Borrelly by the Miniature Integrated Camera and Spectrometer aboard Deep Space 1. *Science* **296**, 1087–1091.
- SUNSHINE, J. M., O. GROUSSIN, P. H. SCHULTZ, M. F. A'HEARN, L. M. FEAGA, T. L. FARNHAM, AND K. P. KLAASEN 2007. The distribution of water ice in the interior of comet Tempel 1. *Icarus* **190**, 284–294.

WING, R. F. 1967. *Infrared Spectrophotometry of Red Giant Stars*. PhD thesis U. C. Berkeley.